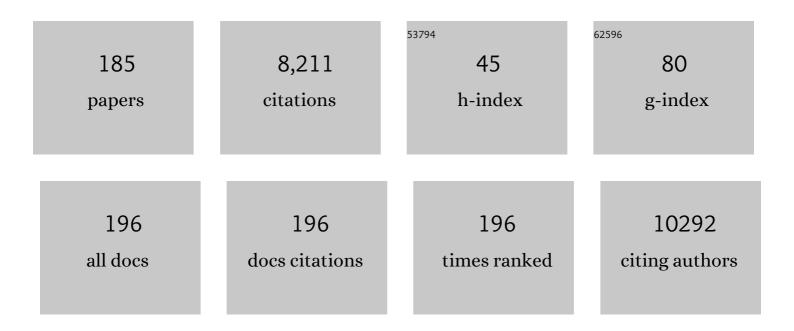
Danny J J Wang

List of Publications by Year in descending order

Source: https://exaly.com/author-pdf/2797314/publications.pdf Version: 2024-02-01



#	Article	IF	CITATIONS
1	Recommended implementation of arterial spinâ€labeled perfusion MRI for clinical applications: A consensus of the ISMRM perfusion study group and the European consortium for ASL in dementia. Magnetic Resonance in Medicine, 2015, 73, 102-116.	3.0	1,663
2	Vascular dysfunction—The disregarded partner of Alzheimer's disease. Alzheimer's and Dementia, 2019, 15, 158-167.	0.8	454
3	Applications of arterial spin labeled MRI in the brain. Journal of Magnetic Resonance Imaging, 2012, 35, 1026-1037.	3.4	272
4	Test–retest reliability of arterial spin labeling with common labeling strategies. Journal of Magnetic Resonance Imaging, 2011, 33, 940-949.	3.4	214
5	Multi-delay multi-parametric arterial spin-labeled perfusion MRI in acute ischemic stroke — Comparison with dynamic susceptibility contrast enhanced perfusion imaging. NeuroImage: Clinical, 2013, 3, 1-7.	2.7	180
6	The Value of Arterial Spin-Labeled Perfusion Imaging in Acute Ischemic Stroke. Stroke, 2012, 43, 1018-1024.	2.0	151
7	Default Mode Network Complexity and Cognitive Decline in Mild Alzheimer's Disease. Frontiers in Neuroscience, 2018, 12, 770.	2.8	103
8	Functional connectivity in BOLD and CBF data: Similarity and reliability of resting brain networks. NeuroImage, 2015, 106, 111-122.	4.2	102
9	Postischemic Hyperperfusion on Arterial Spin Labeled Perfusion MRI is Linked to Hemorrhagic Transformation in Stroke. Journal of Cerebral Blood Flow and Metabolism, 2015, 35, 630-637.	4.3	98
10	Massively parallel functional photoacoustic computed tomography of the human brain. Nature Biomedical Engineering, 2022, 6, 584-592.	22.5	97
11	Cerebral blood flow changes associated with different meditation practices and perceived depth of meditation. Psychiatry Research - Neuroimaging, 2011, 191, 60-67.	1.8	96
12	Multi-delay arterial spin labeling perfusion MRI in moyamoya disease–comparison with CT perfusion imaging. European Radiology, 2014, 24, 1135-1144.	4.5	93
13	Reliability of twoâ€dimensional and threeâ€dimensional pseudoâ€continuous arterial spin labeling perfusion MRI in elderly populations: Comparison with 15oâ€water positron emission tomography. Journal of Magnetic Resonance Imaging, 2014, 39, 931-939.	3.4	93
14	Potentials and Challenges for Arterial Spin Labeling in Pharmacological Magnetic Resonance Imaging. Journal of Pharmacology and Experimental Therapeutics, 2011, 337, 359-366.	2.5	91
15	Neurophysiological Basis of Multi-Scale Entropy of Brain Complexity and Its Relationship With Functional Connectivity. Frontiers in Neuroscience, 2018, 12, 352.	2.8	90
16	Longitudinal Reproducibility and Accuracy of Pseudo-Continuous Arterial Spin–labeled Perfusion MR Imaging in Typically Developing Children. Radiology, 2012, 263, 527-536.	7.3	86
17	Quantitative characterization of nuclear overhauser enhancement and amide proton transfer effects in the human brain at 7 tesla. Magnetic Resonance in Medicine, 2013, 70, 1070-1081.	3.0	85
18	Brain arteriolosclerosis. Acta Neuropathologica, 2021, 141, 1-24.	7.7	85

#	Article	IF	CITATIONS
19	Mapping water exchange across the blood–brain barrier using 3D diffusionâ€prepared arterial spin labeled perfusion MRI. Magnetic Resonance in Medicine, 2019, 81, 3065-3079.	3.0	80
20	Consensus-based technical recommendations for clinical translation of renal ASL MRI. Magnetic Resonance Materials in Physics, Biology, and Medicine, 2020, 33, 141-161.	2.0	80
21	Altered resting perfusion and functional connectivity of default mode network in youth with autism spectrum disorder. Brain and Behavior, 2015, 5, e00358.	2.2	77
22	Characterizing Resting-State Brain Function Using Arterial Spin Labeling. Brain Connectivity, 2015, 5, 527-542.	1.7	75
23	Reduced regional cerebral blood flow in patients with heart failure. European Journal of Heart Failure, 2017, 19, 1294-1302.	7.1	75
24	Arterial spin labeling MRI is able to detect early hemodynamic changes in diabetic nephropathy. Journal of Magnetic Resonance Imaging, 2017, 46, 1810-1817.	3.4	73
25	Multi-vendor reliability of arterial spin labeling perfusion MRI using a near-identical sequence: Implications for multi-center studies. NeuroImage, 2015, 113, 143-152.	4.2	72
26	In vivo venous blood <i>T</i> ₁ measurement using inversion recovery trueâ€FISP in children and adults. Magnetic Resonance in Medicine, 2010, 64, 1140-1147.	3.0	69
27	Unenhanced Dynamic MR Angiography: High Spatial and Temporal Resolution by Using True FISP–based Spin Tagging with Alternating Radiofrequency. Radiology, 2010, 256, 270-279.	7.3	67
28	A twoâ€stage approach for measuring vascular water exchange and arterial transit time by diffusionâ€weighted perfusion MRI. Magnetic Resonance in Medicine, 2012, 67, 1275-1284.	3.0	66
29	Complexity and synchronicity of resting state blood oxygenation level-dependent (BOLD) functional MRI in normal aging and cognitive decline. Journal of Magnetic Resonance Imaging, 2013, 38, 36-45.	3.4	66
30	Reliability comparison of spontaneous brain activities between BOLD and CBF contrasts in eyes-open and eyes-closed resting states. Neurolmage, 2015, 121, 91-105.	4.2	66
31	Clinical 7 T MRI: Are we there yet? A review about magnetic resonance imaging at ultra-high field. British Journal of Radiology, 2019, 92, 20180492.	2.2	66
32	Quantification Issues in Arterial Spin Labeling Perfusion Magnetic Resonance Imaging. Topics in Magnetic Resonance Imaging, 2010, 21, 65-73.	1.2	63
33	Multiple time scale complexity analysis of resting state FMRI. Brain Imaging and Behavior, 2014, 8, 284-291.	2.1	60
34	Noncontrast dynamic MRA in intracranial arteriovenous malformation (AVM): comparison with time of flight (TOF) and digital subtraction angiography (DSA). Magnetic Resonance Imaging, 2012, 30, 869-877.	1.8	59
35	Simultaneous fMRI–PET of the opioidergic pain system in human brain. NeuroImage, 2014, 102, 275-282.	4.2	59
36	Detecting Static and Dynamic Differences between Eyes-Closed and Eyes-Open Resting States Using ASL and BOLD fMRI. PLoS ONE, 2015, 10, e0121757.	2.5	59

#	Article	IF	CITATIONS
37	Simultaneous multi-slice Turbo-FLASH imaging with CAIPIRINHA for whole brain distortion-free pseudo-continuous arterial spin labeling at 3 and 7 T. NeuroImage, 2015, 113, 279-288.	4.2	57
38	Comparison of non-invasive MRI measurements of cerebral blood flow in a large multisite cohort. Journal of Cerebral Blood Flow and Metabolism, 2016, 36, 1244-1256.	4.3	57
39	How the heart speaks to the brain: neural activity during cardiorespiratory interoceptive stimulation. Philosophical Transactions of the Royal Society B: Biological Sciences, 2016, 371, 20160017.	4.0	55
40	Associations of Resting-State fMRI Functional Connectivity with Flow-BOLD Coupling and Regional Vasculature. Brain Connectivity, 2015, 5, 137-146.	1.7	54
41	Transcranial electrical stimulation modifies the neuronal response to psychosocial stress exposure. Human Brain Mapping, 2014, 35, 3750-3759.	3.6	53
42	The pediatric template of brain perfusion. Scientific Data, 2015, 2, 150003.	5.3	53
43	In-vivo Imaging of Magnetic Fields Induced by Transcranial Direct Current Stimulation (tDCS) in Human Brain using MRI. Scientific Reports, 2016, 6, 34385.	3.3	52
44	Regional cerebral blood flow alterations in obstructive sleep apnea. Neuroscience Letters, 2013, 555, 159-164.	2.1	51
45	Dynamic and static contributions of the cerebrovasculature to the resting-state BOLD signal. NeuroImage, 2014, 84, 672-680.	4.2	51
46	Water Exchange across the Bloodâ€Brain Barrier in Obstructive Sleep Apnea: An MRI Diffusionâ€Weighted Pseudoâ€Continuous Arterial Spin Labeling Study. Journal of Neuroimaging, 2015, 25, 900-905.	2.0	51
47	Effect of high dose isoflurane on cerebral blood flow in macaque monkeys. Magnetic Resonance Imaging, 2014, 32, 956-960.	1.8	49
48	Astrocytic tumour grading: a comparative study of three-dimensional pseudocontinuous arterial spin labelling, dynamic susceptibility contrast-enhanced perfusion-weighted imaging, and diffusion-weighted imaging. European Radiology, 2015, 25, 3423-3430.	4.5	49
49	Regional Correlation between Resting State FDG PET and pCASL Perfusion MRI. Journal of Cerebral Blood Flow and Metabolism, 2013, 33, 1909-1914.	4.3	48
50	Arterial Spin Labeling Magnetic Resonance Imaging Estimation of Antegrade and Collateral Flow in Unilateral Middle Cerebral Artery Stenosis. Stroke, 2016, 47, 428-433.	2.0	48
51	Altered Glutamate and Regional Cerebral Blood Flow Levels in Schizophrenia: A 1H-MRS and pCASL study. Neuropsychopharmacology, 2017, 42, 562-571.	5.4	46
52	MarkVCID cerebral small vessel consortium: II. Neuroimaging protocols. Alzheimer's and Dementia, 2021, 17, 716-725.	0.8	45
53	Multi-delay ASL can identify leptomeningeal collateral perfusion in endovascular therapy of ischemic stroke. Oncotarget, 2017, 8, 2437-2443.	1.8	44
54	Turbo-FLASH Based Arterial Spin Labeled Perfusion MRI at 7 T. PLoS ONE, 2013, 8, e66612.	2.5	43

#	Article	IF	CITATIONS
55	Application of arterial spin labeling perfusion MRI to differentiate benign from malignant intracranial meningiomas. European Journal of Radiology, 2017, 97, 31-36.	2.6	42
56	Associations between cerebral blood flow and structural and functional brain imaging measures in individuals with neuropsychologically defined mild cognitive impairment. Neurobiology of Aging, 2020, 86, 64-74.	3.1	42
57	Estimation of perfusion and arterial transit time in myocardium using freeâ€breathing myocardial arterial spin labeling with navigatorâ€echo. Magnetic Resonance in Medicine, 2010, 64, 1289-1295.	3.0	41
58	Baseline <i>CBF</i> , and <i>BOLD, CBF</i> , and <i>CMRO</i> ₂ fMRI of Visual and Vibrotactile Stimulations in Baboons. Journal of Cerebral Blood Flow and Metabolism, 2011, 31, 715-724.	4.3	41
59	Impaired Cerebrovascular Function in Coronary Artery Disease Patients and Recovery Following Cardiac Rehabilitation. Frontiers in Aging Neuroscience, 2015, 7, 224.	3.4	41
60	Deep Learning Detection of Penumbral Tissue on Arterial Spin Labeling in Stroke. Stroke, 2020, 51, 489-497.	2.0	39
61	Retrospective motion artifact correction of structural MRI images using deep learning improves the quality of cortical surface reconstructions. NeuroImage, 2021, 230, 117756.	4.2	39
62	Measurement of Cerebral White Matter Perfusion Using Pseudocontinuous Arterial Spin Labeling 3T Magnetic Resonance Imaging – an Experimental and Theoretical Investigation of Feasibility. PLoS ONE, 2013, 8, e82679.	2.5	38
63	Measuring human placental blood flow with multidelay 3D GRASE pseudocontinuous arterial spin labeling at 3T. Journal of Magnetic Resonance Imaging, 2018, 47, 1667-1676.	3.4	37
64	Loss of Coherence of Low Frequency Fluctuations of BOLD FMRI in Visual Cortex of Healthy Aged Subjects. Open Neuroimaging Journal, 2011, 5, 105-111.	0.2	36
65	Metric Optimization for Surface Analysis in the Laplace-Beltrami Embedding Space. IEEE Transactions on Medical Imaging, 2014, 33, 1447-1463.	8.9	35
66	Assessing intracranial vascular compliance using dynamic arterial spin labeling. Neurolmage, 2016, 124, 433-441.	4.2	35
67	Goldenâ€ratio rotated stackâ€ofâ€stars acquisition for improved volumetric <scp>MRI</scp> . Magnetic Resonance in Medicine, 2017, 78, 2290-2298.	3.0	35
68	Towards the identification of multi-parametric quantitative MRI biomarkers in lupus nephritis. Magnetic Resonance Imaging, 2015, 33, 1066-1074.	1.8	34
69	Comparison of arterial transit times estimated using arterial spin labeling. Magnetic Resonance Materials in Physics, Biology, and Medicine, 2012, 25, 135-144.	2.0	33
70	Noncontrast enhanced fourâ€dimensional dynamic MRA with golden angle radial acquisition and kâ€space weighted image contrast (KWIC) reconstruction. Magnetic Resonance in Medicine, 2014, 72, 1541-1551.	3.0	33
71	Balanced steady state free precession for arterial spin labeling MRI: Initial experience for blood flow mapping in human brain, retina, and kidney. Magnetic Resonance Imaging, 2013, 31, 1044-1050.	1.8	31
72	Collateral perfusion using arterial spin labeling in symptomatic versus asymptomatic middle cerebral artery stenosis. Journal of Cerebral Blood Flow and Metabolism, 2019, 39, 108-117.	4.3	31

#	Article	IF	CITATIONS
73	Water exchange rate across the bloodâ€brain barrier is associated with CSF amyloidâ€Î² 42 in healthy older adults. Alzheimer's and Dementia, 2021, 17, 2020-2029.	0.8	31
74	Comparison of pulsed and pseudocontinuous arterial spinâ€ŀabeling for measuring CO ₂ â€induced cerebrovascular reactivity. Journal of Magnetic Resonance Imaging, 2012, 36, 312-321.	3.4	30
75	Quantitative mouse renal perfusion using arterial spin labeling. NMR in Biomedicine, 2013, 26, 1225-1232.	2.8	30
76	Comparison Between Blood-Brain Barrier Water Exchange Rate and Permeability to Gadolinium-Based Contrast Agent in an Elderly Cohort. Frontiers in Neuroscience, 2020, 14, 571480.	2.8	30
77	Perfusion shift from white to gray matter may account for processing speed deficits in schizophrenia. Human Brain Mapping, 2015, 36, 3793-3804.	3.6	28
78	Differential diagnosis of mitochondrial encephalopathy with lactic acidosis and stroke-like episodes (MELAS) and ischemic stroke using 3D pseudocontinuous arterial spin labeling. Journal of Magnetic Resonance Imaging, 2017, 45, 199-206.	3.4	28
79	A constrained sliceâ€dependent background suppression scheme for simultaneous multislice pseudoâ€continuous arterial spin labeling. Magnetic Resonance in Medicine, 2018, 79, 394-400.	3.0	28
80	Accelerated noncontrastâ€enhanced 4â€dimensional intracranial MR angiography using goldenâ€angle stackâ€ofâ€stars trajectory and compressed sensing with magnitude subtraction. Magnetic Resonance in Medicine, 2018, 79, 867-878.	3.0	28
81	Hypercapnia increases brain viscoelasticity. Journal of Cerebral Blood Flow and Metabolism, 2019, 39, 2445-2455.	4.3	28
82	Multidelay multiparametric arterial spin labeling perfusion MRI and mild cognitive impairment in early stage Parkinson's disease. Human Brain Mapping, 2019, 40, 1317-1327.	3.6	28
83	Regional association of pCASL-MRI with FDG-PET and PiB-PET in people at risk for autosomal dominant Alzheimer's disease. NeuroImage: Clinical, 2018, 17, 751-760.	2.7	27
84	Single and repeated ketamine treatment induces perfusion changes in sensory and limbic networks in major depressive disorder. European Neuropsychopharmacology, 2020, 33, 89-100.	0.7	27
85	Interhemispheric Cerebral Blood Flow Balance during Recovery of Motor Hand Function after Ischemic Stroke—A Longitudinal MRI Study Using Arterial Spin Labeling Perfusion. PLoS ONE, 2014, 9, e106327.	2.5	26
86	Waveletâ€based regularity analysis reveals recurrent spatiotemporal behavior in restingâ€state fMRI. Human Brain Mapping, 2015, 36, 3603-3620.	3.6	26
87	Reduced perfusion in normalâ€appearing white matter in mild to moderate hypertension as revealed by 3D pseudocontinuous arterial spin labeling. Journal of Magnetic Resonance Imaging, 2016, 43, 635-643.	3.4	26
88	Robust single-shot acquisition of high resolution whole brain ASL images by combining time-dependent 2D CAPIRINHA sampling with spatio-temporal TGV reconstruction. NeuroImage, 2020, 206, 116337.	4.2	26
89	Association of Intensive vs Standard Blood Pressure Control With Cerebral Blood Flow. JAMA Neurology, 2022, 79, 380.	9.0	26
90	Quantification of Network Perfusion in ASL Cerebral Blood Flow Data with Seed Based and ICA Approaches. Brain Topography, 2013, 26, 569-580.	1.8	25

#	Article	IF	CITATIONS
91	Evaluation of Cerebral Blood Flow Measured by 3D PCASL as Biomarker of Vascular Cognitive Impairment and Dementia (VCID) in a Cohort of Elderly Latinx Subjects at Risk of Small Vessel Disease. Frontiers in Neuroscience, 2021, 15, 627627.	2.8	25
92	Instrumental validation of free water, peakâ€width of skeletonized mean diffusivity, and white matter hyperintensities: MarkVCID neuroimaging kits. Alzheimer's and Dementia: Diagnosis, Assessment and Disease Monitoring, 2022, 14, e12261.	2.4	25
93	Quantification of arterial cerebral blood volume using multiphaseâ€balanced SSFPâ€based ASL. Magnetic Resonance in Medicine, 2012, 68, 130-139.	3.0	24
94	ASPECTS-based reperfusion status on arterial spin labeling is associated with clinical outcome in acute ischemic stroke patients. Journal of Cerebral Blood Flow and Metabolism, 2018, 38, 382-392.	4.3	24
95	Characterization of lenticulostriate arteries with high resolution black-blood T1-weighted turbo spin echo with variable flip angles at 3 and 7†Tesla. NeuroImage, 2019, 199, 184-193.	4.2	24
96	Human Placenta Blood Flow During Early Gestation With Pseudocontinuous Arterial Spin Labeling MRI. Journal of Magnetic Resonance Imaging, 2020, 51, 1247-1257.	3.4	23
97	Differences in high-definition transcranial direct current stimulation over the motor hotspot versus the premotor cortex on motor network excitability. Scientific Reports, 2019, 9, 17605.	3.3	22
98	Periprocedural Arterial Spin Labeling and Dynamic Susceptibility Contrast Perfusion in Detection of Cerebral Blood Flow in Patients With Acute Ischemic Syndrome. Stroke, 2013, 44, 664-670.	2.0	20
99	Recommended implementation of arterial spinâ€labeled perfusion MRI for clinical applications: A consensus of the ISMRM perfusion study group and the European consortium for ASL in dementia. Magnetic Resonance in Medicine, 2015, 73, spcone.	3.0	19
100	Cerebral Hemodynamic and White Matter Changes of Type 2 Diabetes Revealed by Multi-TI Arterial Spin Labeling and Double Inversion Recovery Sequence. Frontiers in Neurology, 2017, 8, 717.	2.4	19
101	A review of transcranial direct current stimulation (tDCS) for the individualized treatment of depressive symptoms. Personalized Medicine in Psychiatry, 2019, 17-18, 17-22.	0.1	19
102	Relationships between Cerebral Blood Flow and IQ in Typically Developing Children and Adolescents. Journal of Cognitive Science, 2011, 12, 151-170.	0.2	19
103	Detecting resting-state brain activity by spontaneous cerebral blood volume fluctuations using whole brain vascular space occupancy imaging. NeuroImage, 2014, 84, 575-584.	4.2	18
104	Timeâ€resolved noncontrast enhanced 4â€D dynamic magnetic resonance angiography using multibolus TrueFISPâ€based spin tagging with alternating radiofrequency (TrueSTAR). Magnetic Resonance in Medicine, 2014, 71, 551-560.	3.0	18
105	An Automatic Estimation of Arterial Input Function Based on Multi-Stream 3D CNN. Frontiers in Neuroinformatics, 2019, 13, 49.	2.5	18
106	Serotonin transporter genotype modulates the association between depressive symptoms and amygdala activity among psychiatrically healthy adults. Psychiatry Research - Neuroimaging, 2011, 193, 161-167.	1.8	17
107	Patterns of postictal cerebral perfusion in idiopathic generalized epilepsy: a multi-delay multi-parametric arterial spin labelling perfusion MRI study. Scientific Reports, 2016, 6, 28867.	3.3	17
108	Voxelwise Spectral Diffusional Connectivity and Its Applications to Alzheimer's Disease and Intelligence Prediction. Lecture Notes in Computer Science, 2013, 16, 655-662.	1.3	17

#	Article	IF	CITATIONS
109	Phaseâ€cycled simultaneous multislice balanced SSFP imaging with CAIPIRINHA for efficient banding reduction. Magnetic Resonance in Medicine, 2016, 76, 1764-1774.	3.0	16
110	Noncontrastâ€enhanced timeâ€resolved 4D dynamic intracranial MR angiography at 7T: A feasibility study. Journal of Magnetic Resonance Imaging, 2018, 48, 111-120.	3.4	16
111	Eigenanatomy: Sparse dimensionality reduction for multi-modal medical image analysis. Methods, 2015, 73, 43-53.	3.8	15
112	Multi-phase 3D arterial spin labeling brain MRI in assessing cerebral blood perfusion and arterial transit times in children at 3T. Clinical Imaging, 2019, 53, 210-220.	1.5	15
113	Layer-dependent multiplicative effects of spatial attention on contrast responses in human early visual cortex. Progress in Neurobiology, 2020, 207, 101897.	5.7	15
114	Robust functional mapping of layer-selective responses in human lateral geniculate nucleus with high-resolution 7T fMRI. Proceedings of the Royal Society B: Biological Sciences, 2020, 287, 20200245.	2.6	14
115	Cerebroarterial pulsatility and resistivity indices are associated with cognitive impairment and white matter hyperintensity in elderly subjects: A phase-contrast MRI study. Journal of Cerebral Blood Flow and Metabolism, 2021, 41, 670-683.	4.3	14
116	Cerebral perfusion is associated with blast exposure in military personnel without moderate or severe TBI. Journal of Cerebral Blood Flow and Metabolism, 2021, 41, 886-900.	4.3	14
117	Cortical responses to amphetamine exposure studied by pCASL MRI and pharmacokinetic/pharmacodynamic dose modeling. NeuroImage, 2013, 68, 75-82.	4.2	13
118	Decomposing cerebral blood flow MRI into functional and structural components: A non-local approach based on prediction. NeuroImage, 2015, 105, 156-170.	4.2	13
119	Noise Reduction in Arterial Spin Labeling Based Functional Connectivity Using Nuisance Variables. Frontiers in Neuroscience, 2016, 10, 371.	2.8	13
120	Value of pituitary gland MRI at 7 T in Cushing's disease and relationship to inferior petrosal sinus sampling: case report. Journal of Neurosurgery, 2019, 130, 347-351.	1.6	13
121	Dynamics of the cerebral blood flow response to brief neural activity in human visual cortex. Journal of Cerebral Blood Flow and Metabolism, 2020, 40, 1823-1837.	4.3	13
122	Fast Local Trust Region Technique for Diffusion Tensor Registration Using Exact Reorientation and Regularization. IEEE Transactions on Medical Imaging, 2014, 33, 1005-1022.	8.9	12
123	Developmental trajectories of cerebral blood flow and oxidative metabolism at baseline and during working memory tasks. Neurolmage, 2016, 134, 587-596.	4.2	12
124	A longitudinal study of cerebral blood flow under hypoxia at high altitude using 3D pseudo-continuous arterial spin labeling. Scientific Reports, 2017, 7, 43246.	3.3	12
125	Imbalance of Functional Connectivity and Temporal Entropy in Resting-State Networks in Autism Spectrum Disorder: A Machine Learning Approach. Frontiers in Neuroscience, 2018, 12, 869.	2.8	12
126	In-vivo imaging of targeting and modulation of depression-relevant circuitry by transcranial direct current stimulation: a randomized clinical trial. Translational Psychiatry, 2021, 11, 138.	4.8	12

#	Article	IF	CITATIONS
127	Concurrent Imaging of Markers of Current Flow and Neurophysiological Changes During tDCS. Frontiers in Neuroscience, 2020, 14, 374.	2.8	11
128	Optimization of adiabatic pulses for pulsed arterial spin labeling at 7 tesla: Comparison with pseudo ontinuous arterial spin labeling. Magnetic Resonance in Medicine, 2021, 85, 3227-3240.	3.0	11
129	Laminar perfusion imaging with zoomed arterial spin labeling at 7 Tesla. Neurolmage, 2021, 245, 118724.	4.2	11
130	Modulation of brain networks during MR-compatible transcranial direct current stimulation. NeuroImage, 2022, 250, 118874.	4.2	11
131	Quantification of liver perfusion using multidelay pseudocontinuous arterial spin labeling. Journal of Magnetic Resonance Imaging, 2016, 43, 1046-1054.	3.4	10
132	Quantification of intracranial arterial blood flow using noncontrast enhanced 4D dynamic MR angiography. Magnetic Resonance in Medicine, 2019, 82, 449-459.	3.0	10
133	Lower retinal capillary density in minimal cognitive impairment among older Latinx adults. Alzheimer's and Dementia: Diagnosis, Assessment and Disease Monitoring, 2020, 12, e12071.	2.4	10
134	Optimization of pseudoâ€continuous arterial spin labeling at 7T with parallel transmission B1 shimming. Magnetic Resonance in Medicine, 2022, 87, 249-262.	3.0	10
135	High-Resolution Neurovascular Imaging at 7T. Magnetic Resonance Imaging Clinics of North America, 2021, 29, 53-65.	1.1	9
136	Pathophysiological Mechanisms Underlying Idiopathic Normal Pressure Hydrocephalus: A Review of Recent Insights. Frontiers in Aging Neuroscience, 2022, 14, 866313.	3.4	9
137	Recent Advances in Pediatric Brain, Spine, and Neuromuscular Magnetic Resonance Imaging Techniques. Pediatric Neurology, 2019, 96, 7-23.	2.1	8
138	Cerebrovascular reactivity deficits in cognitively unimpaired older adults: vasodilatory versus vasoconstrictive responses. Neurobiology of Aging, 2022, 113, 55-62.	3.1	8
139	Reperfusion Into Severely Damaged Brain Tissue Is Associated With Occurrence of Parenchymal Hemorrhage for Acute Ischemic Stroke. Frontiers in Neurology, 2020, 11, 586.	2.4	7
140	Prospective motion correction for 3D GRASE pCASL with volumetric navigators. Proceedings of the International Society for Magnetic Resonance in Medicine Scientific Meeting and Exhibition., 2017, 25, 0680.	0.5	7
141	Multi-vendor and multisite evaluation of cerebrovascular reactivity mapping using hypercapnia challenge. NeuroImage, 2021, 245, 118754.	4.2	7
142	Selective vulnerability of medial temporal regions to short-term blood pressure variability and cerebral hypoperfusion in older adults. NeuroImage Reports, 2022, 2, 100080.	1.0	7
143	Detection of hyperperfusion on arterial spin labeling using deep learning. , 2015, 2015, 1322-1327.		5
144	Integrated SSFP for functional brain mapping at 7 T with reduced susceptibility artifact. Journal of Magnetic Resonance, 2017, 276, 22-30.	2.1	5

#	Article	IF	CITATIONS
145	Lowâ€dose <scp>CT</scp> perfusion with projection view sharing. Medical Physics, 2018, 45, 101-113.	3.0	5
146	ICâ€₽â€059: REVEALING SMALL SUBFIELDS OF HIPPOCAMPUS IN VIVO WITH 7T STRUCTURAL MRI. Alzheimer's a Dementia, 2018, 14, P55.	and 0.8	5
147	7-Tesla MRI of the brain in a research subject with bilateral, total knee replacement implants: Case report and proposed safety guidelines. Magnetic Resonance Imaging, 2019, 57, 313-316.	1.8	5
148	Low Dose CT Perfusion With K-Space Weighted Image Average (KWIA). IEEE Transactions on Medical Imaging, 2020, 39, 3879-3890.	8.9	5
149	Assessment of carotid stiffness by measuring carotid pulse wave velocity using a singleâ€slice obliqueâ€sagittal phaseâ€contrast MRI. Magnetic Resonance in Medicine, 2021, 86, 442-455.	3.0	5
150	A novel technique for accurate electrode placement over cortical targets for transcranial electrical stimulation (tES) clinical trials. Journal of Neural Engineering, 2021, 18, .	3.5	5
151	Super-Resolution Arterial Spin Labeling Using Slice-Dithered Enhanced Resolution and Simultaneous Multi-Slice Acquisition. Frontiers in Neuroscience, 2021, 15, 737525.	2.8	5
152	Anterior cingulate GABA levels predict whole-brain cerebral blood flow. Neuroscience Letters, 2014, 561, 188-191.	2.1	4
153	Multi-phase passband balanced SSFP fMRI with 50 ms sampling rate at 7 Tesla enables high precision in resolving 100 ms neuronal events. Magnetic Resonance Imaging, 2017, 35, 20-28.	1.8	4
154	Changes in Cerebral Blood Flow during an Alteration in Glycemic State in a Large Non-human Primate (Papio hamadryas sp.). Frontiers in Neuroscience, 2017, 11, 49.	2.8	4
155	Quantification of Load Dependent Brain Activity in Parametric N-Back Working Memory Tasks using Pseudo-continuous Arterial Spin Labeling (pCASL) Perfusion Imaging. Journal of Cognitive Science, 2011, 12, 129-149.	0.2	4
156	Noncontrast Pediatric Brain Perfusion. Magnetic Resonance Imaging Clinics of North America, 2021, 29, 493-513.	1.1	4
157	DTâ€02â€05: MARKVCID PHASE II: PRIORITIZED CANDIDATE SMALL VESSEL VCID BIOMARKERS SELECTED FOR INDEPENDENT MULTIâ€6ITE TESTING AND VALIDATION. Alzheimer's and Dementia, 2018, 14, P1670.	0.8	3
158	Improved sensitivity of cellular MRI using phase-cycled balanced SSFP of ferumoxytol nanocomplex-labeled macrophages at ultrahigh field. International Journal of Nanomedicine, 2018, Volume 13, 3839-3852.	6.7	3
159	Editorial: Advances in Multi-Scale Analysis of Brain Complexity. Frontiers in Neuroscience, 2020, 14, 337.	2.8	3
160	Highly Accelerated SSFP Imaging with Controlled Aliasing in Parallel Imaging and integrated-SSFP (CAIPI-iSSFP). Investigative Magnetic Resonance Imaging, 2017, 21, 210.	0.4	2
161	Fast Diffusion Tensor Registration with Exact Reorientation and Regularization. Lecture Notes in Computer Science, 2012, 15, 138-145.	1.3	2
162	Cerebral perfusion and neurological examination characterise neonatal opioid withdrawal syndrome: a prospective cohort study. Archives of Disease in Childhood: Fetal and Neonatal Edition, 2021, , fetalneonatal-2021-322192.	2.8	2

#	Article	IF	CITATIONS
163	Semiautomatic cerebrovascular territory mapping based on dynamic ASL MR angiography without vesselâ€encoded labeling. Magnetic Resonance in Medicine, 2021, 85, 2735-2746.	3.0	2
164	Multiâ€echo balanced <scp>SSFP</scp> with a sequential phaseâ€encoding order for functional <scp>MR</scp> imaging at <scp>7T</scp> . Magnetic Resonance in Medicine, 0, , .	3.0	2
165	P2â€369: MEASURING WATER EXCHANGE ACROSS BLOOD BRAIN BARRIER IN ELDERLY SUBJECTS BY DIFFUSION WEIGHTED PSEUDOâ€CONTINUOUS ARTERIAL SPIN LABELING. Alzheimer's and Dementia, 2018, 14, P835.	0.8	1
166	Water exchange across bloodâ€brain barrier is associated with CSF amyloidâ€42 level in healthy older adults. Alzheimer's and Dementia, 2020, 16, e036794.	0.8	1
167	fMRI complexity is associated with tauâ€PET and cognitive decline in Alzheimer's disease. Alzheimer's and Dementia, 2020, 16, e045411.	0.8	1
168	Single-Subject Structural Networks with Closed-Form Rotation Invariant Matching Improve Power in Developmental Studies of the Cortex. Lecture Notes in Computer Science, 2014, 17, 137-144.	1.3	1
169	Abstract WP60: Kernel Spectral Regression and Neural Networks Enable Regional Detection of Hemorrhagic Transformation on Multi-Modal MRI for Acute Ischemic Stroke. Stroke, 2018, 49, .	2.0	1
170	P2â€100: IMPACT OF HYPERTENSION ON INTRACRANIAL ARTERIAL COMPLIANCE IN A LATINO COHORT. Alzheimer's and Dementia, 2018, 14, P706.	0.8	0
171	O5â€01â€06: HIGH RESOLUTION 3D BLACK BLOOD MRI OF HUMAN LENTICULOSTRIATE ARTERIES AS AN IMAGIN BIOMARKER FOR VASCULAR COGNITIVE IMPAIRMENT AND DEMENTIA. Alzheimer's and Dementia, 2018, 14, P1641.	IG 0.8	0
172	ICâ€Pâ€085: CHARACTERIZATION OF LENTICULOSTRIATE ARTERIES USING ARTERIAL SPIN LABELING AND HIGHâ€RESOLUTION 3D BLACKâ€BLOOD MRI AS AN IMAGING MARKER IN VASCULAR COGNITIVE IMPAIRMENT AI DEMENTIA. Alzheimer's and Dementia, 2019, 15, P75.	N D. 8	0
173	ICâ€Pâ€041: STRATEGIES OF BRAIN MRI DATA ACQUISITION, QUALITY CONTROL AND ANALYSIS FOR THE MULTICENTER RISK REDUCTION FOR ALZHEIMER'S DISEASE (RRAD) CLINICAL TRIAL. Alzheimer's and Dementia, 2019, 15, P45.	0.8	0
174	Genetic Control Over Cerebral Blood Flow and Resting State Regional Homogeneity Signal. Biological Psychiatry, 2020, 87, S397-S398.	1.3	0
175	Bloodâ€brain barrier dysfunction and perioperative neurocognitive disorders: Cognitive Recovery after Elective Surgery (CREATES) study design and methods. Alzheimer's and Dementia, 2020, 16, e039363.	0.8	0
176	Mean arterial pressure during cerebral perfusion MRI: An arterial spinâ€labeling study in younger and older adults. Alzheimer's and Dementia, 2020, 16, e043623.	0.8	0
177	Detection of attenuated dynamic cerebrovascular function in aging and cognitive decline using a novel neuroimaging approach. Alzheimer's and Dementia, 2020, 16, e045968.	0.8	0
178	Plasma tau is negatively correlated with frontal lobe CBF in hypertensive adults on the AD spectrum. Alzheimer's and Dementia, 2020, 16, e046355.	0.8	0
179	Abstract WP419: Visualization and Evaluation of Human Lenticulostriate Arteries Using High-resolution Black-blood T1-weighted Turbo-spin Echo (TSE) at 3T and 7T. Stroke, 2018, 49, .	2.0	0
180	Abstract WMP24: Reperfusion Into Severely Damaged Brain Tissue is Associated With Impending Parenchymal Hemorrhage in Acute Ischemic Stroke Patients. Stroke, 2018, 49, .	2.0	0

#	Article	IF	CITATIONS
181	Advanced pCASL pediatric perfusion MRI. Advances in Magnetic Resonance Technology and Applications, 2021, , 89-111.	0.1	0
182	k-space weighted image average (KWIA) for ASL-based dynamic MR angiography and perfusion imaging. Magnetic Resonance Imaging, 2022, 86, 94-106.	1.8	0
183	Abstract 13327: Worse Cerebral Blood Flow in Single Right verses Left Ventricle After Fontan Completion. Circulation, 2020, 142, .	1.6	0
184	Editorial for "Multiâ€planar, multiâ€contrast and multiâ€time point analysis tool (<scp>MOCHA</scp>) for intracranial vessel wall characterizationâ€: Journal of Magnetic Resonance Imaging, 2022, 56, 956-957.	3.4	0
185	Effects of Repetitive Peripheral Sensory Stimulation in the Subacute and Chronic Phases After Stroke: Study Protocol for a Pilot Randomized Trial. Frontiers in Neurology, 2022, 13, 779128.	2.4	0